Journal of Engineering Science and Technology
Vol. 12, No. 9 (2017) 2488 - 2503

ESTIMATION OF THE SPECIFIC ENERGY OF TUNNEL BORING MACHINE USING POST-FAILURE BEHAVIOUR OF ROCK MASS.CASE STUDY: KARAJ-TEHRAN WATER CONVEYANCE TUNNEL IN IRAN

MAJID MIRAHMADI[1*], MORTEZA TABEEI[2], MOHSEN S. DEHKORDI[3]

[1]Department of Geology, Payam Noor University, PO BOX 19395-3697 Tehran, Iran
[2]Department of Mining Engineering, Isfahan University of Technology, Isfahan 84156-83111. Iran
[3]Department of Civil Engineering, Islamic Azad University, Bafgh Branch, Bafgh, Iran
*Corresponding Author: m.mirahmadi@mi.iut.ac.ir

Abstract

Performance prediction of tunnel boring machines (TBM) is the most important factor for successful tunnel excavation projects. The specific energy (SE) of TBM, defined as the amount of energy required to excavate a unit volume of rock, is one of the critical parameters used for performance prediction of these machines. Estimation of SE is very useful to design the drilling project because it is a function of many parameters such as rock mass behaviour, machine properties and project parameters. Several methods are used to estimate this parameter, such as experimental, empirical and numerical. The aim of this study is to estimate the SE considering the post-failure behaviour of rock mass. For this reason, based on the actual data from Karaj-Tehran water conveyance tunnel, a new empirical method is proposed to estimate the SE using the drop-to-deformation modulus ratio (λ). Based on the statistical analysis, the relation between the SE and λ is estimated. It is clear that the amplitude of λ, is high and to increase the correlation between mentioned parameters, the classification of data is performed. All data is classified in three classes as very weak (GSI<25) to very good classes (GSI>75). Also a statistical analysis is performed to estimate the SE using the mentioned parameter (λ) in any class. The result shows that there is a direct relation between both parameters and the best correlation is achieved. So, the best equations are proposed to estimate SE using λ, considering the post-failure behaviour of rock mass.

Keywords: Specific energy, Drop modulus, Deformation modulus, Post-failure behaviour.

Nomenclatures

E	Deformation modulus, GPa
F	Thrust, kN
F_C	Cutting force, kN
F_R	Rolling force, kN
M	Drop modulus, GPa
N	Cutter head rotation speed, rps
P	Power of cutter head of the machine, kW
Q	Yield, m^3/km
SE_{des}	Destruction specific energy, MJ/m^3
T	Torque, kNm
u	Average rate of advance, m/s

Greek Symbols

σ	Stress, MPa
ε	Strain
η	Softening parameter
$\lambda/$	Drop to deformation modulus ratio

Abbreviations

GSI	Geological strength index
IPR	Instantaneous penetration rate, m/hr
SE	Specific energy of TBM, MJ/m^3
TBM	Tunnel boring machine

1. Introduction

Tunnel boring machines (TBMs) are used to excavate in nearly all rock masses and under varying geological conditions ranging from soft ground and soil to hard rocks. TBMs have become an alternative to traditional methods such as drill and blast. The advantages of these machines include the rapid excavation and advance rates compared to alternative methods, while offering a safe working condition. Performance prediction of TBMs and the determination of some design parameters have become crucial, as they are critical elements in planning a project of mechanical excavation. Error in performance estimation can result in project delays and cost overruns as seen in many case histories [1]. Intact rock properties together with rock mass characteristics should be well investigated for selection of proper TBM for tunnelling in various ground conditions. This is due to the significant impact of rock mass characteristics on machine performance. TBMs are site specific and designed for optimal performance in given ground conditions. When selected and put to work at a specific site, TBM parameters including thrust and torque are the controlling factors for excavation rate. These two parameters along with rock properties and rock mass characteristics converge to define the operating point of a machine [2].

The specific energy of excavation (SE) is defined as the amount of energy required to excavate a unit volume of rock mass (MJ/m^3). The concept of SE has been presented first time by Teale (1965) in the petroleum industry, and is a parameter for assessing the efficiency of drilling processes and excavation in rock

masses. SE can be determined in real time by the data recording the performance of a drilling machine or a TBM. Boyd (1986) calculated rate of penetration based on SE of rock mass [3]. In addition, what makes this parameter particularly attractive is its correlation with the mechanical properties of the rock mass [4]. Some researchers such as Hustrulid [5] and Muirhead and Glossop [6] and proposed that there was a good correlation between uniaxial compressive strength (UCS) and SE. Altindag [7] found a significant association, with high correlation coefficients, between SE and the brittleness of rock mass. Bieniawski et al. [8] found correlation between Rock Mass Excavability and SE. Acaroglu et al. [4] established a model to predict SE requirement of constant cross-section disc cutters in the rock cutting process by fuzzy logic method. Atici and Ersoy [9] estimated the effect of brittleness and destruction energy on SE. Zhang et al. [10] established an identification model of SE by introducing the mechanical analysis of the shield excavating process into the nonlinear multiple regression of the on-site data. Wang et al. [11] developed new SE equations with change in disc cutter radius. In the next section, the concept and applications of SE are explained.

2. Concept of Specific Energy

Specific energy is defined as the energy consumed to complete the excavation of unit volume of rock mass [10]. In practice, the SE is a useful parameter to estimate the energy requirements for a particular cutting operation. The SE value can be calculated by the forces imposed on disc cutters, and the forces on disc cutters can be estimated using TBM operation parameters [11]. SE includes two components, the first of which arises from the rolling force of the disc cutter. The other component arises from the thrust force of the disc cutter. A schematic model of working TBM and forces is presented in Fig. 1. As illustrated, the machine is being driven by both the thrust (F) and the torque (T) during tunnelling. Therefore, the energy is mainly consumed on the thrust to constantly push the machine forward and the torque to maintain continuously rotating the cutter head to cut the rock mass. In fact, the required thrust is spent to generate the micro fractures in rock mass. In other words, the thrust force is related to pre-failure section of complete stress-strain curve of rock mass. Post-failure behaviour of rock mass indicates the value of required torque because it is spent to propagate micro fracture and create macro fracture.

Teale [12] proposed SE as the following Eq. (1):

$$SE = \left(\frac{F}{A}\right) + \left(\frac{2\pi}{A}\right)\left(\frac{NT}{u}\right) \quad (1)$$

where SE is specific energy of excavation (MJ/m^3); F is total cutter head thrust (kN); A is excavated face area (m^2); N is cutter head rotation speed (rps); T is applied torque (kNm); and u is average rate of advance (m/s).

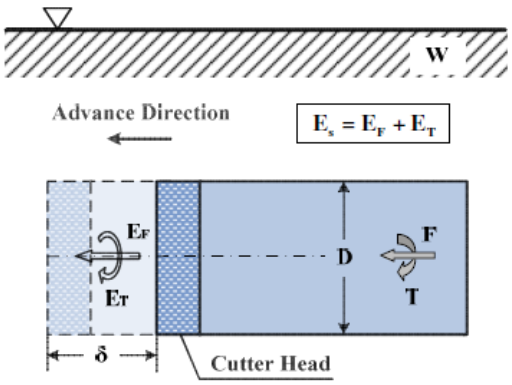

Fig. 1. Schematic representation of the working process of a shield machine [10].

Equation (1) has two terms, the first representing the SE of the cutter head thrust from static loading, while the second term is the SE of rotation incurred by the rotating cutter head.

Acaroglu et al. (2008) proposed that SE was a function of rolling force (F_R) and the area of the cutting profile as seen in Eq. (2) [13]:

$$SE = \frac{F_R.R.t}{V} = \frac{F_R}{A} \quad (2)$$

where *SE* is the specific energy (kWh/m^3); F_R is the rolling force (kN); *R* is the velocity of cutting (m/s); *t* is the cutting time (s); *V* is the volume of the excavated rock (m^3); and *A* is the profile area of the cutting which is a function of the cutting penetration and spacing between cuts.

Cutting forces which can also be used as performance parameters of disc cutters are shown in Fig. 1. Using the SE value obtained from Eq. (1), Instantaneous Penetration Rate (*IPR*) of TBMs can be estimated by Eq. (3):

$$\text{IPR} = \frac{\text{P.K}}{\text{SE.A}_\text{t}} \quad (3)$$

where *IPR* is the instantaneous penetration rate (m/hr); *P* is the power of cutter head of the machine (kW); *SE* is the specific energy (kWh/m^3); *k* is the mechanical efficiency factor; and A_t is the tunnel area (m^2).

SE is also used for estimation and comparison of cutting efficiency (production rates) of mechanized systems and as one of the most important factors for defining their optimum cutting geometries (optimum ratio of depth of cut to line spacing) for a given rock sample [14]. *SE* is estimated as shown in Eq. (4) [15]:

$$SE = \frac{FC}{Q} \quad (4)$$

where *SE* is specific energy (MJ/m^3); *FC* is the cutting force acting on the tool (kN); and *Q* is the yield or rock volume cut in unit cutting length (m^3/km).

Theoretically the *SE* value is equal to area under the complete stress-strain curve in unconfined compression test, as illustrated in Fig. 2 [9]. In a brittle failure mode, rocks break with very little or no deformation but in a plastic failure rock needs to

deform elastically until it yields, and plastic deformation occurs until rupture. The failure behaviour of brittle and of ductile rock masses is completely different (Fig. 2). From the physical point of view, the integral of the envelope curve is an energy (or work) related to the volume. Since this is the work required for drilling of the rock mass, this property is defined as *SE* for drilling. As a product of both stress–strain and SE, the work of shape altering is calculated including the post-failure section. Whereas the deformation modulus submits the gradient (derivation) of linear section, it is derived from the following Eq. (5) [9]:

$$SE = \int \sigma . d\varepsilon \tag{5}$$

where SE is the specific energy (kJ/m^3), σ is the stress (MPa), and ε is the strain.

In the next section, the concept of drop modulus of rock mass is explained.

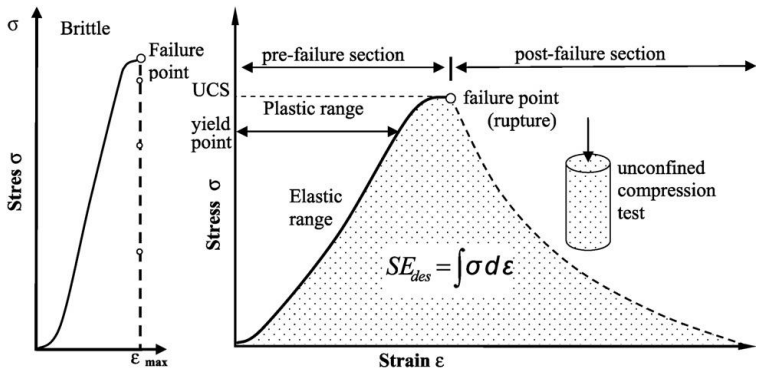

Fig. 2. Estimation of the destruction specific energy (SEdes) from the stress–strain curve of a rock sample under unconfined compression test [9].

3. Concept of Drop Modulus

Hoek and Brown [16] suggested guidelines to estimate the post-failure behaviour types of rock mass according to rock mass quality. As seen in Fig. 3, these guidelines are based on rock types:

a) For very good quality hard rock masses, with a high geological strength index (GSI) (GSI>75), the rock mass behaviour is elastic brittle;

b) For averagely jointed rock (25<GSI<75), moderate stress levels result in a failure of joint systems and the rock becomes gravely, strain softening behaviour is assumed;

c) For very weak rock (GSI<25), the rock mass behaves in an elastic perfectly plastic manner and no dilation is assumed and behaviour is perfectly plastic.

The strain softening behaviour can accommodate purely brittle behaviour and elastic perfectly plastic behaviour, so brittle and elastic perfectly plastic behaviours are special cases of the strain softening behaviour [17]. Strain softening behaviour is characterized by a gradual transition from a peak to a residual failure criterion that is governed by the softening parameter, η [18]. In this model when the softening parameter is null, an elastic regime exists, and whenever $0 < \eta < \eta^*$, the softening

regime occurs and the residual state takes place when $\eta > \eta*$, with $\eta*$, defined as the value of the softening parameter controlling the transition between the softening and residual stages. This model is illustrated in Fig. 4.

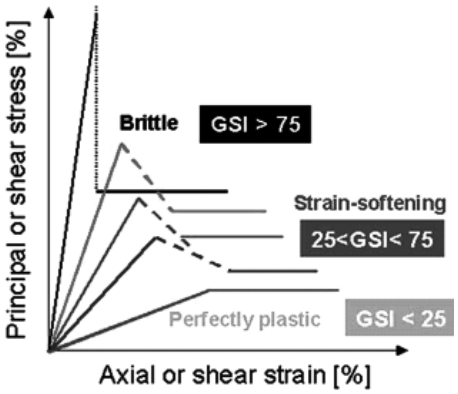

Fig. 3. Different post-failure behaviour modes for rock masses with different geological strength indices [19].

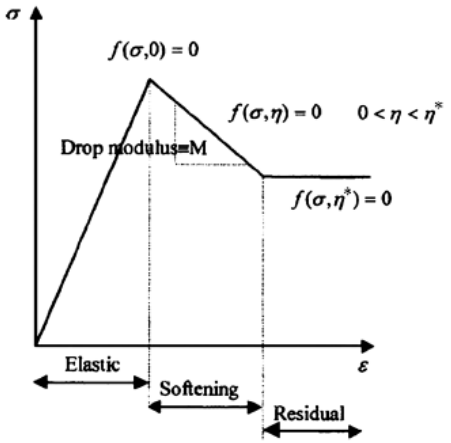

Fig. 4. Stress-strain curve for an unconfined test performed on a sample of strain softening material [19].

It is obvious that perfectly brittle or elastic–brittle–plastic and perfectly plastic models are special cases of the strain softening model. The following information is needed to characterize a strain softening rock mass: (1) Peak and residual failure criteria, (2) elastic parameters (Young's modulus and Poisson's ratio), and (3) post-failure deformability parameters. Joints, micro-cracks, and groundwater reduce strength of rock mass. The GSI, as a scaling parameter is used to provide an estimate of the decreased rock mass strength based on the Hoek-Brown criterion [20]. The GSI is an empirically dimensionless number that varies over a range between 10 and 100. By definition, GSI values close to 10 correspond to very-poor quality rock mass while GSI values close to 100 correspond to excellent-quality rock masses [16, 21-23]. When the GSI scale factor is introduced, the Hoek–Brown failure criterion for the rock mass is given as follows Eq. (6) [24]:

$$\sigma_1 = \sigma_3 + \sigma_{ci}\,(m_b.\frac{\sigma_3}{\sigma_{ci}} + s)^a \quad (6)$$

The parameter m_b in Eq. (6) depends on the following parameters: the intact rock parameter, m_i, the value of GSI, and disturbance factor *D*, as defined by the next Eq. (7) [22, 25]:

$$m_b = m_i . exp(\frac{GSI-100}{28-14D}) \quad (7)$$

D is a factor which depends upon the degree of disturbance to which the rock mass has been subjected by blast damage and stress relaxation. It varies from 0 for undisturbed in situ rock masses to 0.8 for very disturbed rock masses in tunnels [16, 22, 25]. The parameter, s, depends empirically on the value of GSI and D as follows Eq. (8) [16, 22, 25]:

$$S = exp(\frac{GSI-100}{9-3D}) \quad (8)$$

The parameter, a, also depends empirically on the value of GSI, as follows Eq. (9) [22]:

$$a = \frac{1}{2} + \frac{1}{6}(e^{\frac{-GSI}{15}} - e^{\frac{-20}{3}}) \quad (9)$$

Determining the appropriate value of σ_3 for use in Eq. (6) is very important because the confinement stress affects rock mass behavior as with increasing confinement stress, the rock mass behaviors become more and more ductile and finally behave ideally plastic and with decreasing the confinement stress, the post peak behaviour of rock mass tends to brittle behaviour [17]. The confinement stress is estimated by Eq. (10) [22]:

$$\frac{\sigma_3}{\sigma_{cm}} = 0.47(\frac{\sigma_{cm}}{\gamma.H})^{-0.94} \quad (10)$$

where σ_{cm} is the rock mass strength, defined by Eq. (11), γ is the unit weight of the rock mass, and *H* is the depth of the tunnel below surface. In case the horizontal stress is higher than the vertical stress, the horizontal stress value should be used in place of $\gamma . H$ [22].

$$\sigma_{cm} = \frac{2.c.cos\Phi}{1-sin\Phi} \quad (11)$$

where *C* is the cohesion of rock mass and Φ is the friction angle of rock mass.

In this study, peak properties of rock masses were estimated based on the Hoek and Brown proposal [16].

The slope for the softening stage or drop modulus is denoted by M. If the drop modulus approaches to infinity, perfectly brittle behaviour appears, whereas perfectly plastic behaviour is obtained if this modulus approaches to zero [19]. One of the most important parameters effect on drop modulus is confinement stress, as with increasing this parameter, the rock mass behaviours become more and more ductile and finally behave ideally plastic [26] and drop modulus tends to zero and with decreasing the confinement pressure, the rock mass behaviour tends to brittle and the drop modulus increases to infinite. Carranza-Torres and Fairhurst study [26] showed that ideally plastic behaviour, without strain softening post-failure, may be expected when the confinement pressure, σ_3, is equal to or greater than one-fifth of the axial stress at failure (Fig. 5) [27]. Assuming the failure criterion of Hoek and Brown, based on Seeber's condition, the relationship between the confinement

pressure and the UCS of the intact rock can be obtained [28]. This relationship can be approximated estimated by Eq. (12):

$$\sigma_{3,crit} \geq \frac{\sigma_c . m_b}{16} \tag{12}$$

where m_b is the product of a parameter m depending on the lithology, with a reduction factor depending on the degree of fracturing of the rock.

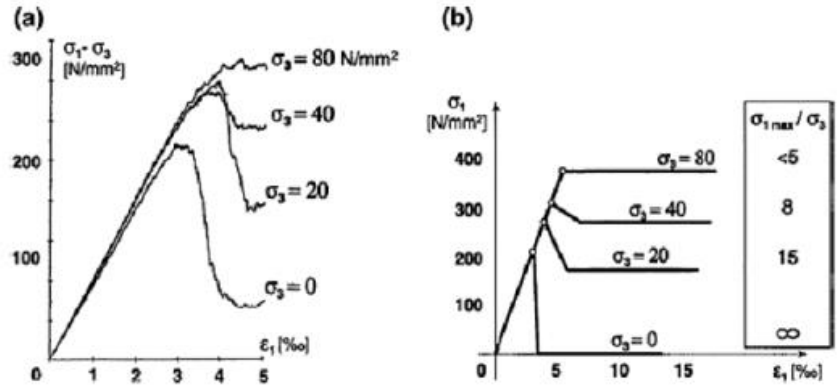

Fig. 5. Dependence of the post-failure behaviour of granite samples on the confinement pressure; (a) Results of a numerical simulation of the 3-axial tests; (b) Schematic behaviour [28].

Estimating approaches of pre and post-failure deformability

The deformation modulus of rock mass is the most important parameter affecting the mechanical behaviour of rock mass. There are several methods to estimate this parameter such as in situ tests, back analysis using numerical methods and empirical equations, which are based on the application of rock mass classifications. Although the best method to estimate this parameter is in situ tests, it is costly and often very difficult. Therefore, determining the modulus of deformation of the rock masses with other methods continues to attract the attention of rock engineers and engineering geologists. Thus, E_{rm} can be generally estimated and easily be acquired by means of empirical methods.

The pre-failure deformability was obtained using empirical approaches. The deformation modulus, E_{rm}, can be obtained from Hoek and Diederichs approach due to using more effective factors on deformability such as the elastic modulus of intact rock, E_i, disturbance factor, D, and GSI in the equation Eq. (13) [29]:

$$E_{rm} = E_i . \left(\frac{1-\frac{D}{2}}{1+e^{\frac{(75+25D-GSI)}{11}}}\right) \tag{13}$$

Poisson's ratio, v, does not usually affect rock behaviour to a significant degree, so standard values in the range of 0.25–0.35 are likely to be valid for any approaches [30].

The deformability post-failure behaviour of rock masses is highly dependent on rock mass quality and confinement stress. Based on these observations, the following values, proposed by Alejano et al. [19] were used to estimate the drop modulus of the rock mass according to the peak rock mass quality determined by

GSI peak and the level of confinement stress expressed in terms of the rock mass compressive strength given by $\sqrt{s^{peak}}.\sigma_{ci}$. The values obtained, thus, take into account the assumption of a continuous trend, from brittle behavior in high-quality rock masses subjected to unconfined conditions to pure ductile behavior in poor-quality rock masses for extremely high confinement stresses. Based on Alenjano et al.'s equations, values of the drop modulus depend on the deformation's modulus, E_{rm}, according to Eq. (14) [19]:

$$M = -\omega.E_{rm} \tag{14}$$

The value of the ratio ω depends on the GSIpeak and confinement stress level, and it can be estimated according to Eqs. (15) and (16):

$$\omega = \left[0.0046e^{0.0768.GSI^{peak}}\right]\left(\frac{\sigma_3}{\sqrt{s^{peak}}.\sigma_{ci}}\right)^{-1} \; for \; \frac{\sigma_3}{\sqrt{s^{peak}}.\sigma_{ci}} \geq 0.1 \tag{15}$$

$$\omega = \left[0.0046e^{0.0768.GSI^{peak}}\right]\left(\frac{\sigma_3}{2\sqrt{s^{peak}}.\sigma_{ci}} + 0.05\right)^{-1} \quad for \; \frac{\sigma_3}{\sqrt{s^{peak}}.\sigma_{ci}} \leq 0. \tag{16}$$

If confinement stresses are not considered in calculation, the drop modulus can be estimated according to Eq. (17) [19]:

$$M = \frac{E_{rm}}{0.08.GSI-7} \qquad For \quad 25 < GSI < 75 \tag{17}$$

A more complex approach to estimating drop modulus, including the effect of σ_{ci} , is Eq. (18) [19]:

$$\mathrm{M} = \frac{E_{rm}}{0.0812\left(GSI+\frac{\sigma_{ci(MPa)}}{10}\right)-7.66} \qquad For \quad 20 < GSI < 75 \tag{18}$$

The following Eq. (19) is used as the first approach to estimating the drop modulus if one uses more complex strain softening models with confinement stress being dependent on drop modulus [19]:

$$M = \frac{1ooo.E}{GSI.\,\sigma_3+75.GSI-225\;\sigma_3-5875} \qquad \text{For} \quad 5 < GSI < 75 \tag{19}$$

The most complex equation to estimate the drop modulus is defined in Eq. (20):

$$M = \frac{E_{rm}}{1-\left[\left[\frac{8.66-0.0812\,.\left(GSI+\,\sigma_{ci(MPa)}\right)}{8-0.08\,.GSI}\right].\left[\left(\frac{225-GSI}{1000}\right).\sigma_3+\left(\frac{55-0.6GSI}{8}\right)\right]\right]} \tag{20}$$

Equation (20), which is used for GSI ranging from 20 to 75, applies more effective factors such as GSI, confinement stress, σ_3, unixial strength of intact rock, $\sigma_{ci,}$, etc. [19].

All mentioned equations were used to estimate the drop modulus in this study.

4. Project's Description and Geology

Karaj-Tehran Water Conveyance Tunnel is one of the components of a water management system in Iran which is designed for transfer 16 (m^3/s) of water from Amir-Kabir dam to Refinery No.6 in Tehran. Total length of tunnel is 30 km and divided into two sections. The Lot 2 with 14 km in length and 4.66 m in diameter is excavated with a double shield TBM Herrenknecht Model S323. The basic specifications of utilized TBM are shown in Table 1 [31].

The tunnel alignment contains a series of asymmetric faults and folded formations. The lithology of this area consists of a sequence of Karaj formations and a variety of pyroclastic rocks, often interbedded with sedimentary rocks. The characteristic rock types in this section are gray tuff, siltstone, sandstone, monzo-diorite and monzo-gabbro.

Table 1. Technical specifications of double shield TBM Herrenknecht Model S323 [32-34].

Excavation machine type	Double shield TBM
Length of machine	166m
Length of Shield	10.6m
Weight of machine	750 ton
Weight of Shield	170 ton
Weight of cutter head	45 ton
Number of disc cutters	31
Average Spacing of disc cutters	75mm
Max.cutterhead thrust (kN)	17000
Cutterhead torque (kN.m)	2500
Cutterhead speed (RPM)	0 to 11
Cutters diameter (mm)	432

This tunnel is located on the Chaloos road, about 35 km west of Tehran. In Fig. 6, the location and route of tunnel are shown.

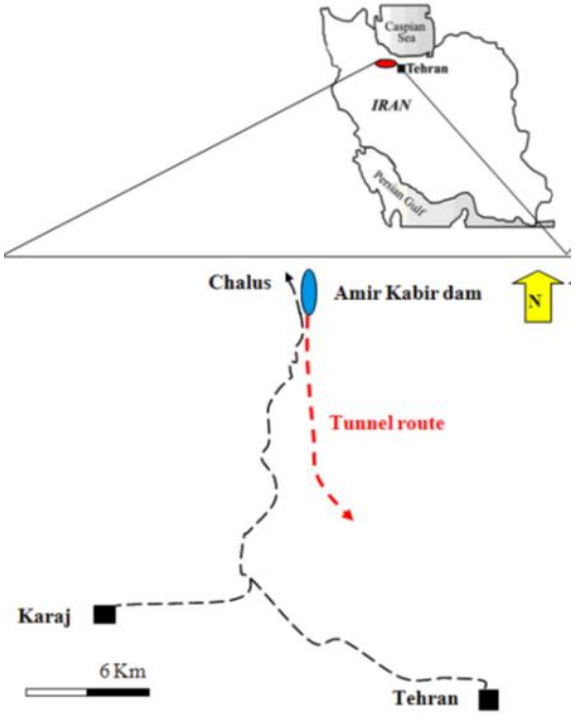

Fig. 6. Location and route of Karaj-Tehran water conveyance tunnel [34].

In general, by considering the repeated units in different parts of the tunnel route, 20 engineering geological units were distinguished. Geological and geomechanical properties of rock mass types are mentioned in Table 2.

Table 2. Geo-mechanical properties of engineering geological units of tunnel.

Engineering geological units	Sign	GSIPeak	σ_{ci}(MPa)	σ_{cm} (MPa)	E_{rm}(GPa)
Diorite	DIO	65-75	100-200	61.7	15
Gabbro	GA	60-70	100-200	57.4	12.5
Lithic crystal tuff	LCT	40-50	50-100	15.2	5
Ash and lithic tuff	AL	35-45	50-100	13.7	4
Lithic and lapili tuff	LL	60-70	50-100	32.6	7.5
Lapili tuff	LT	50-60	50-100	16.2	5
Gabbro rubble	BG	55-65	50-75	17.1	7.5
Thick lithic tuff	LC	50-60	100-150	31.2	7.5
Lithic and ash tuff	LA	55-65	50-100	20.8	7.5
Massive lipili tuff	MLT	50-60	50-100	26.3	5
Monzonite	MO	70-80	100-200	69.3	15
Gray tuff	GT	50-60	50-100	16.6	5
Lithic lapili tuff	LLT	65-75	100-150	43.5	10
Ash tuff	AT	35-45	50-100	8.8	2.5
Cream tuff	CT	70-80	100-150	44.5	10
Gray lithic tuff	GLT	45-55	50-100	22.5	5
Green and cream tuff	TU	45-55	100-150	24.7	7.5
Ash lithic tuff	ALT	40-50	50-100	9.9	4
Fractured zone	FZ	20-30	---	8.1	2.5
Crushed zone	CZ	15-25	---	6.3	1.5

5. Estimating of Specific Energy in Different Post-Failure Behaviour of Rock Mass

In this section based on actual data collected from Karaj-Tehran water conveyance tunnel the absolute value of the drop to deformation modulus ratio (λ) was estimated according to the next Eq. (21):

$$\lambda = \left|\frac{M}{E_{rm}}\right| \quad (21)$$

The drop modulus was estimated using the mentioned equations in previous section. The maximum and minimum λ, varying between 0.009176186 15.44491116, depends on quality of rock mass and confinement stress, so that an increase in the confinement stress and a decrease in quality of rock mass can cause decrease in λ, representing a truly inverse correlation.

Based on the statistical analysis, the maximum correlation between the two parameters is achieved using Eqs. (14), (15) and (16) to estimate the drop modulus.

In the next step, the classification of rock mass, with regard to the geological strength index, proposed Hoek and Brown [16], is performed and as seen in Table

3, all data are classified in three classes as very weak (GSI<25) to very good classes (GSI>75) and the statistical analysis to estimate the SE is performed in any class.

Table 3. Rock mass classification based on GSI.

GSI	Engineering geological units	Post failure behaviour
25> GSI	FZ-CZ	Perfectly Plastic
25<GSI<75	GA-LCT-AL-LL-LT-BG-LC-LA-MLT-GT-LLT-AT-GLT-TU-ALT	Strain Softening
GSI>75	DIO-MO-CT	Brittle

5.1. Estimating of specific energy in very weak rock mass (GSI<25)

As mentioned above with decreasing the quality of rock mass and increasing the confinement stress, the drop to deformation modulus ratio tended to zero and the behaviour of rock mass changed to elastic–plastic. In this class (GSI<25), the quality of rock mass was very weak and the rock mass behaviour was elastic-perfectly plastic. Based on the regression analysis, there was a direct relation between both parameters and the best correlation was achieved by logarithmic equation, shown in Fig. 7. The following Eq. (22) was achieved to estimate the SE:

$$SE = 4.6089 \ln(\lambda) + 34.912 \quad (22)$$

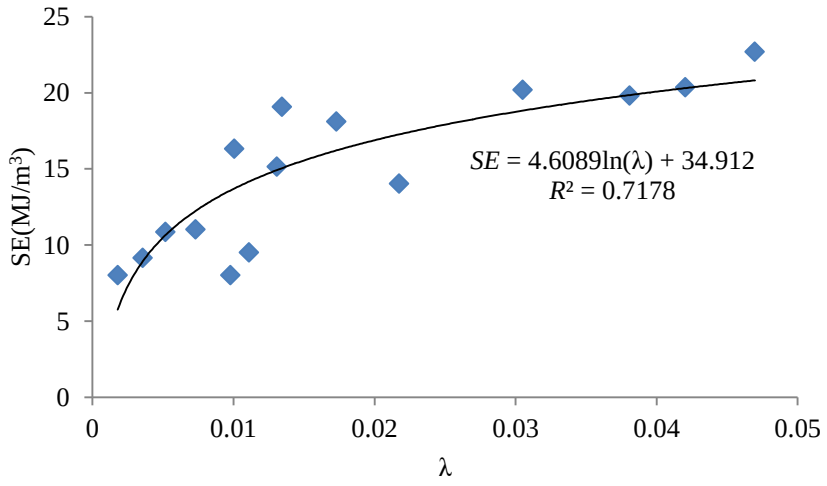

Fig. 7. The relationship between the drop to deformation modulus ratio and specific energy in very weak rock mass (GSI <25).

5.2. Estimating of specific energy in favourable rock mass (25< GSI< 75)

In this class ($25 < GSI < 75$), the condition of rock mass was favour and good and the rock mass behaviour was elastic–strain softening and the SE increased. Based on the regression analysis, there was a direct correlation between both parameters and the power equation was proposed to estimate the SE (according to Fig. 8). The next Eq. (23) was achieved to estimate SE:

$$SE = 36.589\lambda^{0.179} \quad (23)$$

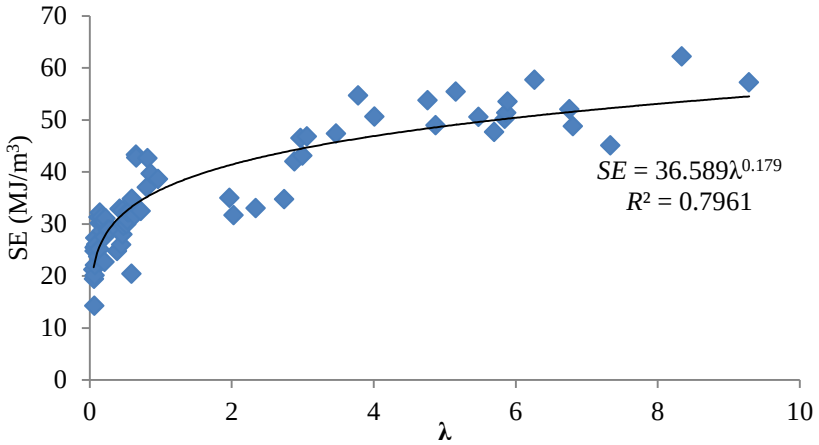

Fig. 8. The relationship between the drop to deformation modulus ratio and specific energy in favourable rock mass (25<GSI<75).

5.3. Estimating of specific energy in good rock mass (GSI >75)

It is clear that increasing the quality of rock mass and decreasing the confinement stress caused the drop to deformation modulus ratio to tend to infinity and the behaviour of rock mass to change to elastic–brittle. The rock mass condition of this class was good and the rock mass behaviour tends to elastic–brittle to elastic–perfectly brittle and the SE was very high. According to Fig. 9, there was a direct relationship between the drop to deformation modulus ratio and SE and the polynomial equation was proposed to estimate the SE. The Eq. (24) was achieved to estimate the SE:

$$SE = 0.0101\lambda^2 + 1.2633\lambda + 53.915 \quad (24)$$

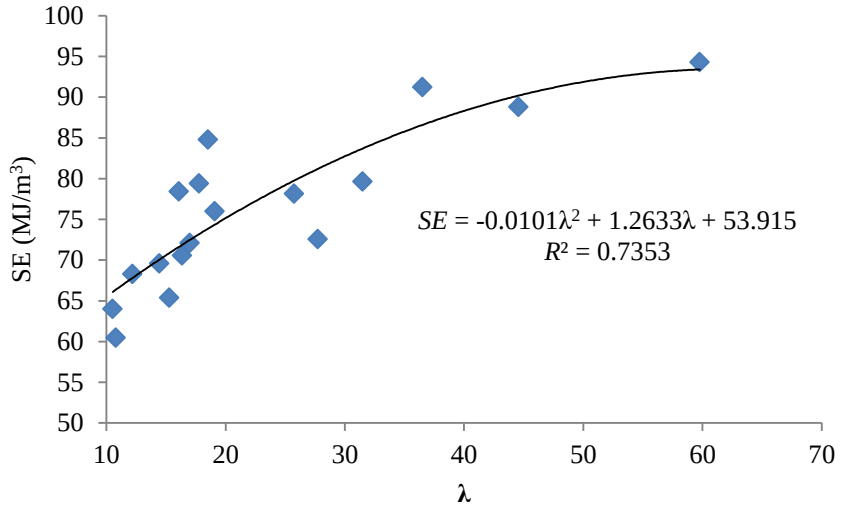

Fig. 9. The relationship between the drop to deformation modulus ratio and specific energy in good rock mass (GSI > 75).

6. Conclusions

In this study, estimation of the specific energy is done considering the post-failure behaviour of rock mass. For this reason, using statistical analysis based on the actual data from Karaj-Tehran water conveyance tunnel, a new empirical method is proposed to estimate SE using the drop to deformation modulus ratio (called λ)

- The strain softening behaviour can accommodate purely brittle behaviour and elastic perfectly plastic behaviour, so brittle and elastic perfectly plastic behaviours are special cases of the strain softening behaviour. Reasonably it is strongly capable of representing the macroscopic results commonly observed in practice.
- The results of model showed that increasing the quality of rock mass and decreasing the minimum principal stress can cause increase in the drop to deformation modulus ratio (λ), because the rock mass behaviour changes from elastic plastic to elastic brittle and drop modulus intends to infinite, representing a truly inverse relationship.
- Based on the statistical analysis, the maximum correlation was achieved using Equations 14-16 to estimate the drop modulus.
- Finally, the relationship between the SE and the drop to deformation modulus ratio, λ, in different post-failure behaviour of rock mass was estimated. It is clear that the amplitude of λ is high, and to increase the correlation between the mentioned parameters, the classification of data is performed and all data are classified into three classes [according to the proposed classification by Hoek and Brown [16] as very weak (GSI<25) to very good classes (GSI>75). Also, a statistical analysis was performed to estimate the SE using the mentioned parameter (λ) in any class. The result showed that there is a direct relation between both parameters and the best equation was achieved for each class. Finally, it is emphasized that the empirical relationship should not be used alone for designing.

References

1. Ghasemi, E.; Yagiz, S.; and Ataei, M. (2014). Predicting penetration rate of hard rock tunnel boring machine using fuzzy logic. *Bulletin of Engineering Geology and the Environment*, 73(1), 23-35.
2. Yagiz, S.; Rostami, J.; Kim, T.; Ozdemir, L.; and Merguerian, C. (2009). Factors influencing performance of hard rock tunnel boring machines. *ISRM Regional Symposium-EUROCK* 2009, International Society for Rock Mechanics.
3. Hassanpour, J.; Rostami, J.; Azali, S.T., and Zhao, J. (2014). Introduction of an empirical TBM cutter wear prediction model for pyroclastic and mafic igneous rocks; a case history of Karaj water conveyance tunnel, Iran. *Tunnelling and Underground Space Technology*, 43, 222-231.
4. Acaroglu, O.; Ozdemir, L.; and Asbury, B. (2008). A fuzzy logic model to predict specific energy requirement for TBM performance prediction. *Tunnelling and Underground Space Technology*, 23(5), 600-608.
5. Hustrulid, W.A. (1972). Comparison of laboratory cutting results and actual tunnel boring performance. Rapid Excavation And Tunneling Conference.
6. Muirhead, I.; and Glossop, L. (1968). *Hard rock tunnelling machines*. https://trid.trb.org/view.aspx?id=123306.

7. Altindag, R. (2003). Correlation of specific energy with rock brittleness concepts on rock cutting. *Journal of the South African Institute of Mining and Metallurgy*, 103(3), 163-171.
8. Bieniawski, Z.; Celada, B.; Galera, J.; and Tardaguila, I. (2008). New applications of the excavability index for selection of TBM types and predicting their performance. *ITA-AITES World Tunnel Congress & 34th ITA General Assembly*. Agra, India.
9. Atici, U.; and Ersoy, A. (2009). Correlation of specific energy of cutting saws and drilling bits with rock brittleness and destruction energy. *Journal of Materials Processing Technology*, 209(5), 2602-2612.
10. Zhang, Q.; Qu, C.; Cai, Z.; Huang, T.; Kang, Y.; Hu, M.; Dai, B.; and Leng, J. (2012). Modeling specific energy for shield machine by non-linear multiple regression method and mechanical analysis. *Proceedings of the 2011 2nd International Congress on Computer Applications and Computational Science*, 1, 75-80.
11. Wang, L.; Kang, Y.; Cai, Z.; Zhang, Q.; Zhao, Y.; Zhao, H.; and Su, P. (2012). The energy method to predict disc cutter wear extent for hard rock TBMs. *Tunnelling and Underground Space Technology*, 28, 183-191.
12. Teale, R. (1965). The concept of specific energy in rock drilling. In: *International Journal of Rock Mechanics and Mining Sciences & Geomechanics Abstracts*, 1, 57-73.
13. Acaroglu, O. (2011). Prediction of thrust and torque requirements of TBMs with fuzzy logic models. *Tunnelling and Underground Space Technology*, 26(2), 267-275.
14. Bilgin, N.; Copur, H.; and Balci, C. (2013). *Mechanical Excavation in Mining and Civil Industries*. USA: CRC Press, Taylor & Francis Group.
15. Roxborough, F.F.; and Phillips, H.R. (1975). Rock excavation by disc cutter. *International Journal of Rock Mechanics and Mining Sciences & Geomechanics Abstracts*, 12, 361-366.
16. Hoek, E.; and Brown, E. (1997). Practical estimates of rock mass strength. *International Journal of Rock Mechanics and Mining Sciences*, 34(8), 1165-1186.
17. Alejano, L.; Rodriguez-Dono, A.; Alonso, E.; and Fdez-Manin, G. (2009). Ground reaction curves for tunnels excavated in different quality rock masses showing several types of post-failure behaviour. *Tunnelling and Underground Space Technology*, 24(6), 689-705.
18. Dehkordi, M.S.; Lazemi, H.; Shahriar, K.; and Dehkordi M.S. (2015). Estimation of the rock load in non-squeezing ground condition using the post failure properties of rock mass. *Geotechnical and Geological Engineering*, 33(4), 1115-1128.
19. Alejano, L.; Alonso, E.; Rodriguez-Dono, A.; and Fernandez-Manin, G. (2010). Application of the convergence-confinement method to tunnels in rock masses exhibiting Hoek–Brown strain-softening behaviour. *International Journal of Rock Mechanics and Mining Sciences*, 47(1), 150-160.
20. Dehkordi, M.S.; Shahriar, K.; Moarefvand, P.; and Gharouninik, M. (2013). Application of the strain energy to estimate the rock load in squeezing ground condition of Eamzade Hashem tunnel in Iran. *Arabian Journal of Geosciences*, 6(4), 1241-1248.

21. Tutluoğlu, L.; Öge, İ.F. and Karpuz. C. (2015). Relationship between pre-failure and post-failure mechanical properties of rock material of different origin. *Rock Mechanics and Rock Engineering*, 48(1), 121-141.
22. Hoek, E.; Carranza-Torres, C.; and Corkum, B. (2002). Hoek-Brown failure criterion-2002 edition. *Proceedings of NARMS-Tac Conferences*. Toronto, Canada, 267-273.
23. Cai, M.; Kaiser, P.; Uno, H.; Tasaka, Y.; and Minami, M. (2004). Estimation of rock mass deformation modulus and strength of jointed hard rock masses using the GSI system. *International Journal of Rock Mechanics and Mining Sciences*, 41(1), 3-19.
24. Hoek, E.; Carranza-Torres, C.; Diederichs, M.; and Corkum, B. (2008). The 2008 kersten lecture integration of geotechnical and structural design in tunneling. *56th Annual Geotechnical Engineering Conference*. St. Paul. Minnesota, 1-53.
25. Rummel, F.; and Fairhurst, C. (1970). Determination of the post-failure behavior of brittle rock using a servo-controlled testing machine. *Rock mechanics*, 2(4), 189-204.
26. Carranza-Torres, C.; and Fairhurst, C. (2000). Application of the convergence-confinement method of tunnel design to rock masses that satisfy the Hoek-Brown failure criterion. *Tunnelling and Underground Space Technology*, 15(2), 187-213.
27. Egger, P. (2000). Design and construction aspects of deep tunnels (with particular emphasis on strain softening rocks). *Tunnelling and Underground Space Technology*, 15(4), 403-408.
28. Hoek, E.; and Diederichs, M.S. (2006). Empirical estimation of rock mass modulus. *International Journal of Rock Mechanics and Mining Sciences*, 43(2), 203-215.
29. Dehkordi, M.S.; Shahriar, K.; Maarefvand, P.; and Gharouninik, M. (2011). Application of the strain energy to estimate the rock load in non-squeezing ground condition. *Archives of Mining Sciences*, 56, 551-566.
30. Frough, O.; and Torabi, S.R. (2013). An application of rock engineering systems for estimating TBM downtimes. *Engineering Geology*, 157, 112-123.
31. Dehkordi, M.S.; Lazemi, H.;and Shahriar, K. (2015). Application of the strain energy ratio and the equivalent thrust per cutter to predict the penetration rate of TBM, case study: Karaj-Tehran water conveyance tunnel of Iran. *Arabian Journal of Geosciences*, 8, 4833-4842.
32. Hassanpour, J.; Rostami, J.; Khamehchiyan, M.; Bruland, A.; and Tavakoli, H. (2010). TBM performance analysis in pyroclastic rocks: a case history of Karaj water conveyance tunnel. *Rock Mechanics and Rock Engineering*, 43(4), 427-445.
33. Salimi, A.; and Esmaeili, M. (2013). Utilising of linear and non-linear prediction tools for evaluation of penetration rate of tunnel boring machine in hard rock condition. *International Journal of Mining and Mineral Engineering*, 4(3), 249-264.
34. Khanlari, G.; and Mokhtari, E. (2012). Engineering geological study of the second part of water supply Karaj to Tehran tunnel with emphasis on squeezing problems. *Engineering Geology*, 145-146, 9-17.